Digital Documentation of the Ain Akrine Archaeological Site (Lebanon): A Hybrid UAV Photogrammetry and SLAM-Based Survey Approach

Eleonora Maset[1], Riccardo Valente[2], May Haider[3], Marco Iamoni[4]

[1] Polytechnic Department of Engineering and Architecture (DPIA), University of Udine, Udine, Italy – eleonora.maset@uniud.it
[2] Institute of Heritage Science (ISPC), National Research Council, Milano, Italy – riccardo.valente@cnr.it
[3] Lebanese University, 3rd Branch Tripoli, Lebanon – may.haider@ul.edu.lb
[4] Department of Humanities and Cultural Heritage (DIUM), University of Udine, Udine, Italy – marco.iamoni@uniud.it

Keywords: SLAM-based portable laser scanning, UAV photogrammetry, Multi-sensor survey, 3D point cloud integration, Cultural heritage documentation

Abstract

Digital access to archaeological and cultural heritage sites is increasingly important for research, conservation, and public dissemination. This paper presents a hybrid survey strategy combining Unmanned Aerial Vehicle (UAV) photogrammetry and Portable Laser Scanning (PLS) based on Simultaneous Localization and Mapping (SLAM) technology for the documentation of the Ain Akrine archaeological site (Koura region, northern Lebanon), a vegetated hilltop area hosting the Roman Qasr Naous temples. The proposed multi-sensor approach enables the generation of site-scale orthophotos and surface models, detailed photogrammetric reconstructions of the temples, and a SLAM-derived point cloud providing continuous coverage of the entire area, including densely vegetated zones. The integration of multiple PLS acquisitions with photogrammetric datasets results in a spatially consistent and multi-scale 3D representation. Quantitative accuracy analyses confirm the high reliability of the photogrammetric products and demonstrate that the SLAM-based survey achieves accuracy levels consistent with the expected performance of the adopted sensor, despite the absence of external constraints. The results highlight the effectiveness and flexibility of hybrid UAV–PLS approaches for comprehensive archaeological documentation under challenging environmental and logistical conditions.

1. Introduction

Providing digital access to archaeological and Cultural Heritage (CH) sites is increasingly important to promote global awareness, facilitate research, and support conservation. Digital documentation enables scholars and professionals to analyze remote or fragile sites without physical interaction, contributing to their long-term preservation, while also allowing a wider audience to virtually explore heritage assets that are often difficult to access (Mendoza et al., 2023). However, meeting these requirements strongly depends on the availability of effective and reliable three-dimensional (3D) surveying techniques. In recent years, rapid technological advancements have significantly improved mapping capabilities, fostering the adoption of lightweight, portable, and user-friendly instruments specifically suited to complex CH environments (Zlot et al., 2014).

Among these technologies, Unmanned Aerial Vehicle (UAV)-based photogrammetry has become a well-established and widely adopted approach for CH documentation, thanks to its high geometric accuracy, rich radiometric content, and flexibility in capturing large areas from above (Pepe et al., 2022). When supported by robust topographic control, it can deliver accurate orthophotos, dense point clouds, and detailed 3D models. However, its applicability is not without limitations. Dense vegetation can significantly reduce ground visibility, while flight restrictions, safety regulations, and environmental constraints may limit UAV operations. In addition, the need for well-distributed, topographically measured Ground Control Points (GCPs) can be problematic in remote, forested, or logistically constrained archaeological contexts. Alternatively, the reliance on Global Navigation Satellite System (GNSS)–Real Time Kinematic (RTK) positioning for direct image georeferencing may also be limited in such environments.

In parallel, Portable Laser Scanning (PLS) systems based on Simultaneous Localization and Mapping (SLAM) technology have emerged as a powerful alternative for rapid terrestrial data acquisition (Di Stefano et al., 2021). Handheld SLAM-based systems enable continuous 3D mapping without the need for GNSS signals or extensive control networks, allowing operators to efficiently survey large, complex, and vegetated areas with minimal setup time (Hess and Ferreyra, 2021, Maté-González et al., 2022, Fassi et al., 2025). Nevertheless, SLAM-based surveys also present specific challenges, including trajectory drift accumulation, variable or reduced point density and higher noise (Conti et al., 2024), and generally lower local geometric accuracy compared to well-constrained photogrammetric or Terrestrial Laser Scanning (TLS) reconstructions (Matellon et al., 2024).

To ensure reliable digital access across scenarios with different morphologies, sizes, and levels of complexity, while accounting for operational and logistical constraints, hybrid multi-sensor survey strategies have proven to be especially effective for the comprehensive documentation of CH sites (Chiabrando et al., 2019, Masciotta et al., 2023). By combining UAV photogrammetry and PLS, it is possible to achieve both high-detail modelling of architectural remains and complete spatial coverage of extensive and vegetated areas, resulting in integrated 3D representations (Perfetti et al., 2023).

This work builds upon previous methodological investigations (Maset et al., 2022), where a hybrid survey approach, based on photogrammetry and portable laser scanning, was tested on a small archaeological site in northern Lebanon. In the present study, the methodology is validated and extended to a significantly larger and more complex context, namely the Ain Akrine area, located in the Koura region of Lebanon. The hilltop site covers approximately 1.9 hectares and hosts the Roman Qasr Naous temples, representing a challenging environment in terms of extent, topography, and vegetation density. While UAV photogrammetry is treated as a consolidated reference technique, the primary focus of this paper is on the SLAM-based survey, its processing workflow, achievable accuracy, and its integration with photogrammetric data.

The paper is structured as follows. Section 2 introduces the archaeological and geographical context of the case study. Section 3 describes the data acquisition and processing workflow, detailing both the UAV photogrammetric survey and the SLAM-based PLS methodology, including data integration procedures. Section 4 presents and discusses the results, with particular attention to accuracy assessment and multi-sensor data fusion. Finally, Sect. 5 summarizes the main conclusions and outlines perspectives for future applications of hybrid UAV–SLAM surveys in other archaeological contexts.

2. Study Area and Archaeological Context

In the village of Ain Akrine, in the North Governorate of Lebanon, lies the archaeological area of Qasr Naous (Fig. 1(a)). The area was an important religious spot, at least from the Roman period. It covers the top of the hill close to the village of Ain Akrine and overlooks the entire plain (Fig. 1(b)).

(a) Site location.

(b) Hilltop site overview.

Figure 1. (a) Location of the Ain Akrine village in northern Lebanon (Google Satellite basemap). (b) Aerial view of the Qasr Naous archaeological area, located on a hilltop overlooking the surrounding plain.

Two main temples are still extant and clearly visible (Fig. 2(a)). The eastern temple (called also temple B) is in a relatively good state of conservation, with some columns still standing and a large portion of the *cella*. The western temple (called also temple A) is almost completely destroyed, with only the elevated base remaining and partially covered by rubble. Despite its worse conditions, the western temple has a better preserved *temenos*, i.e., the holy perimeter around the temple itself, and has a quite large number of scattered architectural elements. Among these is the only known fragment of sculpture coming from this area, the reproduction of a human chest with a tunic and a sort of *nimbus* that could suggest an identification with Helios. The temples date back to the imperial Roman period. On the northern side of the eastern temple there are the remains of a residential area that are usually considered as what still exists of a medieval village (Renan, 1864-1874, Krencker and Zschietzschmann, 1938, Donceel, 1966, Taylor, 1971, Collart and Coupel, 1977, Nordiguian, 2005, Aliquot, 2009, Iamoni et al., 2019, Iamoni et al., in press).

(a) Eastern and western Roman temples.

(b) Vegetation and terrain complexity.

Figure 2. (a) Close-range aerial views of the eastern (left) and western (right) Roman temples. (b) Terrestrial view of the archaeological area, highlighting ground-level complexity and dense vegetation surrounding and between the architectural remains.

The area between and around the two temples is characterized by dense and irregular vegetation, which partially conceals architectural remains and prevents direct visibility of the ground surface from aerial viewpoints (Fig. 2(b)). This environmental condition represents a significant constraint for aerial-only survey approaches and strongly influences the choice of documentation strategies for the site.

Within this framework, the adopted multi-sensor survey strategy was designed to address two complementary objectives. On the one hand, the documentation of the entire archaeological area was required to capture the overall morphology of the hilltop site and its spatial relationships with the surrounding landscape. On the other hand, high-resolution surveys of the two Roman temples were necessary to accurately document their architectural features and current state of preservation. The combination of site-scale mapping and detailed architectural and archaeological documentation represents a key step toward the generation of accurate and comprehensive 3D models, supporting archaeological analysis, site management, and long-term conservation and dissemination activities.

3. Data Acquisition and Processing

3.1 UAV Photogrammetric Survey

The survey campaign was carried out in June 2022 and required two days of fieldwork. A first UAV flight was performed to cover the entire site, using a DJI Mavic 2 Pro equipped with a 20 MP RGB camera (5472 × 3648 pixels). A total of 215 images were acquired, achieving an average Ground Sampling Distance (GSD) of 20 mm. In addition, two close-range UAV surveys were conducted to capture the two temples at a higher level of detail. The eastern temple, better preserved and rich of architectural elements, was documented using 428 images with an average GSD of 3 mm. The western temple, largely collapsed and in a more fragmentary state of preservation, was surveyed through 261 images with an average GSD of 13 mm.

The three photogrammetric datasets were processed separately using 3DF Zephyr software (3Dflow, v. 8.038), applying a standard photogrammetric workflow. Image orientation was performed through a Structure-from-Motion (SfM) approach, followed by dense matching at full image resolution to generate dense point clouds. Subsequently, polygonal surface models were reconstructed and textured meshes were produced for the two temples. The dataset covering the entire site was further used to generate an orthophoto and a Digital Surface Model (DSM), providing a comprehensive overview of the area.

High geometric accuracy of the SfM-based reconstruction was ensured through the use of GCPs measured with a Leica TS03 total station. Due to the extent of the site, a topographic control network composed of 15 survey stations was established in order to measure all targets distributed across the area. Overall, 30 targets were surveyed. Considering target visibility within the different image blocks, 14 GCPs were used for the processing of the site-scale dataset, while 5 and 6 GCPs were employed for the eastern and western temple datasets, respectively. The remaining surveyed points were used as independent Check Points (CPs) to assess the accuracy of the photogrammetric reconstructions, as discussed in Sect. 4.

A high-precision GNSS survey could not be performed at the site due to logistical and environmental limitations. Therefore, after constraining the photogrammetric solution using the accurately measured GCPs, an additional roto-translation was applied to approximately align the local reference frame to a global coordinate system (WGS84/UTM Zone 36N, EPSG:32636). The transformation parameters were estimated using the approximate coordinates of the UAV camera positions provided by the onboard GNSS receiver, allowing the generation of georeferenced final products.

3.2 SLAM-Based PLS Survey

In addition to photogrammetry, a ground-based survey was carried out using the HERON Lite PLS (Gexcel srl), a handheld mobile mapping system based on SLAM principles. The device employs a 16-channel Velodyne Puck LITE Light Detection and Ranging (LiDAR) sensor, capable of acquiring up to 300,000 points per second. The sensor provides full horizontal coverage (360°) with a 30° vertical field of view and a maximum measurement range of 100 m. To support trajectory estimation, the LiDAR data are combined with measurements from an integrated Xsens MTi Inertial Measurement Unit (IMU). During data acquisition, the scanning unit was mounted on a telescopic carbon-fiber pole, enabling the operator to perform continuous surveys while walking, even in morphologically complex or vegetated zones (Fig. 3).

Figure 3. Operator performing the PLS survey.

Despite the considerable extent of the Qasr Naous site, the PLS survey was completed by a single operator in approximately two hours, covering both temples and the surrounding archaeological area. Data acquisition was carried out through five separate SLAM sessions, whose main characteristics in terms of trajectory length, acquisition time, and point cloud size are reported in Tab. 1. During data acquisition, particular care was taken to ensure sufficient spatial overlap between consecutive SLAM sessions, by planning partially redundant trajectories across the surveyed area. The resulting high degree of overlap among the five sessions played a key role in enabling a robust global registration during the subsequent integration phase. Overall, the SLAM-based survey covered a total trajectory length of 3.15 km.

Acquisition	Trj. length [m]	Time [min:s]	Size num. points
PLS#1	561	15:17	107,112,178
PLS#2	347	11:49	50,363,582
PLS#3	408	12:06	74,855,200
PLS#4	826	18:28	141,598,062
PLS#5	1007	25:50	140,534,865

Table 1. Characteristics of the SLAM-based PLS acquisitions (trajectory length, acquisition time, and number of points in the reconstructed cloud).

Raw LiDAR and IMU measurements were processed using HERON Desktop software (Gexcel srl, v. 2.3.3). Particular attention was devoted to the so-called *global optimization* stage of each session, which performs loop-closure detection and trajectory adjustment in order to mitigate the drift effects that are typically observable in the intermediate steps of the processing pipeline (Maset et al., 2021). This optimization allowed the generation of five internally consistent and geometrically stable point clouds, each corresponding to a single acquisition session, prior to their integration into a unified dataset.

The five SLAM-derived point clouds were subsequently merged using the point cloud registration tools available in JRC 3D Reconstructor software (Gexcel srl, v. 4.3.2). Manual pre-alignment was first applied to roughly position the datasets in a common reference frame. This was followed by pairwise Iterative Closest Point (ICP) registrations to refine the relative alignment between overlapping acquisitions. Finally, a global ICP-based bundle adjustment was performed, simultaneously considering all possible point cloud pairs. This approach introduced additional constraints into the multi-cloud registration problem with respect to incremental pairwise registration, effectively minimizing residual misalignments and improving the overall geometric consistency of the final model. The integrated PLS dataset consists of more than 500 million points, providing a continuous and detailed 3D representation of the entire archaeological area.

Following the integration of the five SLAM-derived point clouds, the resulting PLS data was further processed through point cloud classification. Ground and overground points were automatically classified using TerraScan software (Terrasolid, v. 025), enabling the generation of a Digital Terrain Model (DTM) of the site.

3.3 Multi-Sensor Data Integration

As a final step, the point clouds derived from the different survey techniques were integrated within a common reference system. The complete PLS point cloud was aligned to the site-scale photogrammetric dense cloud using the ICP approach implemented in JRC 3D Reconstructor, allowing all datasets to be brought into a consistent spatial reference. Within the areas occupied by the two temples, the PLS points were removed and replaced with the corresponding high-resolution photogrammetric dense point clouds. The resulting integrated dataset combines continuous site-scale coverage with detailed architectural geometry, yielding a unified point cloud suitable for subsequent analysis and comparison.

4. Results and Discussion

4.1 UAV Photogrammetry Results

The UAV photogrammetric survey produced outputs at multiple spatial scales, supporting both site-scale analysis and detailed documentation of the architectural remains. At the site scale, the generation of a high-resolution orthophoto provides a synoptic two-dimensional overview of the archaeological area and its spatial organization (Fig. 4(a)). The orthophoto enables a clear interpretation of the overall layout of the site, the position of the two temples, and their relationship with the surrounding landscape. In addition, the photogrammetric-derived DSM (Fig. 4(b)) supports the analysis of site morphology and elevation differences across the hilltop area, offering a valuable basis for spatial interpretation at the landscape scale.

At the architectural scale, the close-range UAV acquisitions enabled the reconstruction of high-resolution dense point clouds and detailed textured meshes of the two Roman temples (Fig. 5). These models accurately capture the geometry and surface appearance of the preserved structures, supporting detailed architectural analysis and providing visually effective products for documentation and dissemination purposes. The different levels of detail achieved for the eastern and western temples reflect both their state of preservation and the tailored acquisition strategy adopted for each structure.

The accuracy of the UAV photogrammetric products was assessed using independent CPs measured during the topographic survey and not included in the bundle adjustment. The evaluation was performed separately for the site-scale dataset and for the two close-range temple reconstructions. Table 2 reports the number of CPs used for each dataset, together with

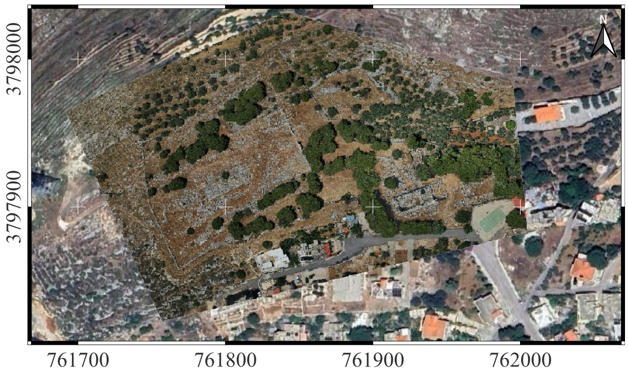

(a) Orthophoto.

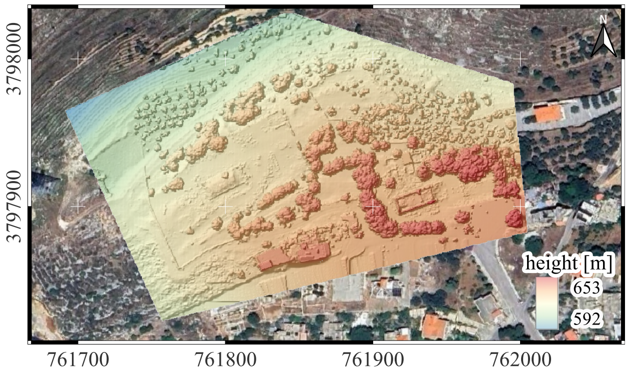

(b) DSM.

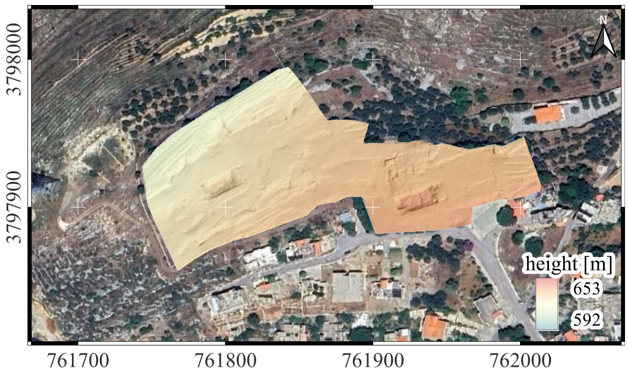

(c) DTM.

Figure 4. (a) UAV-derived orthophoto showing the Ain Akrine archaeological area; (b) Photogrammetric derived DSM; (c) DTM obtained from the SLAM-based PLS survey. The survey products are overlaid on a low-resolution Google Satellite image (WGS84/UTM Zone 36N, EPSG:32636).

the mean vertical error (Mean_Z), the mean three-dimensional error (Mean_{3D}), and the three-dimensional Root Mean Square Error (RMSE_{3D}). The results show a high level of geometric accuracy for all photogrammetric products. At the site scale, the RMSE_{3D} computed on 13 CPs is 0.020 m, with a negligible mean vertical bias ($\text{Mean}_Z = -0.004$ m), indicating a well-constrained bundle adjustment despite the large extent of the surveyed area. The close-range reconstructions of the temples achieve even higher accuracy, with RMSE_{3D} values of 0.015 m and 0.017 m for the eastern and western temples, respectively. These results are consistent with the higher image resolution and more favorable imaging geometry of the close-range UAV surveys.

https://doi.org/10.5194/isprs-archives-XLVIII-2-W12-2026-287-2026


(a) Eastern temple.

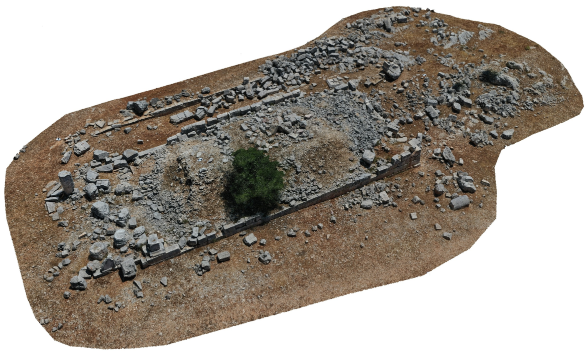
(b) Western temple.

Figure 5. Textured mesh of the temples from the UAV photogrammetric survey.

Surveyed area	CP n. points	Mean$_Z$ [m]	Mean$_{3D}$ [m]	RMSE$_{3D}$ [m]
Entire site	13	-0.004	0.019	0.020
Eastern temple	5	-0.008	0.013	0.015
Western temple	6	0.006	0.014	0.017

Table 2. Errors on CPs.

4.2 SLAM-Based PLS Results

The SLAM-derived PLS dataset provides a complete three-dimensional representation of the archaeological site at the landscape scale. Figure 6(a) shows the final integrated point cloud obtained from the five acquisition sessions, with the individual contributions highlighted using different colors. This visualization allows a clear appreciation of the spatial extent of the survey and of the continuity achieved through the multi-session acquisition strategy. In addition to the 3D point cloud, the PLS survey enabled the generation of an X-ray orthophoto by projecting the point cloud onto a horizontal plane (Fig. 6(b)). This product offers a highly informative and complementary representation with respect to the UAV-derived orthophoto, providing effective two-dimensional representations supporting the analysis of site morphology and site management tasks, even by users without direct access to, or expertise in, 3D point cloud visualization.

One of the main advantages of the SLAM-based approach is the ability to capture ground geometry even in densely vegetated areas. This aspect is clearly illustrated by the vertical cross-sections extracted from the PLS point cloud (Fig. 7), which reveal the underlying terrain morphology beneath tree canopies and in areas not visible from aerial viewpoints. The completeness of the ground sampling provided by the PLS data made it possible to derive a Digital Terrain Model (DTM) of the entire archaeological area (Fig. 4(c)), overcoming the limitations of photogrammetric DSMs for terrain representation in vegetated zones.

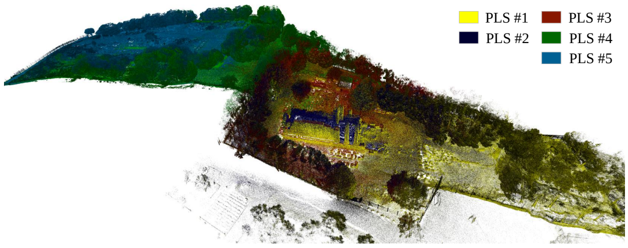

(a) Point cloud.

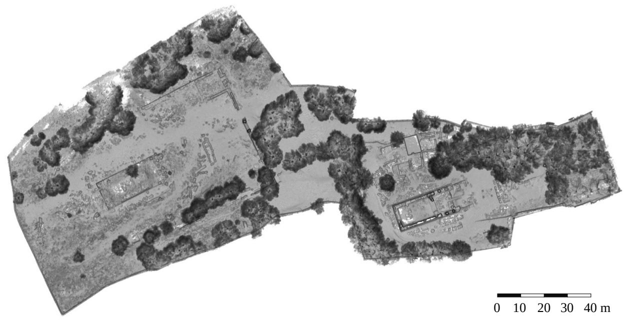

(b) X-ray orthophoto.

Figure 6. Outputs from the SLAM-based PLS survey. (a) The final point cloud, colored according to the five acquisition sessions; (b) X-ray orthophoto, obtained by projecting the point cloud on an horizontal plane.

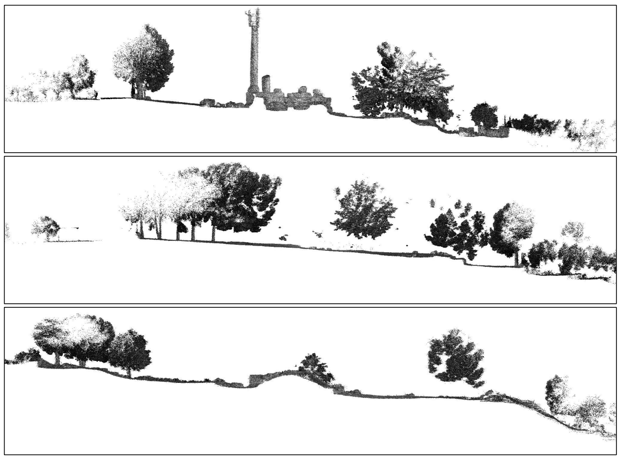

Figure 7. Vertical cross-sections extracted from the SLAM-based point cloud. The site morphology is clearly visible, including areas located behind and among the trees.

The geometric consistency of the SLAM-based PLS dataset was first evaluated during the integration of the five acquisition sessions. The final ICP-based bundle adjustment performed in JRC 3D Reconstructor resulted in a mean residual error of 0.035 m across all point cloud pairs. This value is consistent with the expected performance of the sensor, also considering the extent of the surveyed area, the acquisition strategy, and the challenging environmental conditions of the site.

A global Cloud-to-Cloud (C2C) comparison between the PLS and UAV point clouds was not considered appropriate, as the

https://doi.org/10.5194/isprs-archives-XLVIII-2-W12-2026-287-2026

results would be strongly biased by vegetation and by the lack of ground points beneath dense canopy in the photogrammetric dataset. The site-scale accuracy of the PLS survey was therefore assessed using independently measured topographic points, including both targets used as GCPs and CPs for photogrammetry and additional ground points corresponding to total station setup locations. Since these topographic points could not be directly identified in the SLAM-derived point cloud, the accuracy assessment was performed through a point-to-point comparison in the vertical direction, computing the elevation difference (Z) between each topographic point and its nearest neighbor in the PLS point cloud. The same analysis was applied to the site-scale UAV photogrammetric dense cloud in order to provide a consistent reference. The distributions of the vertical discrepancies are shown in the histograms in Fig. 8.

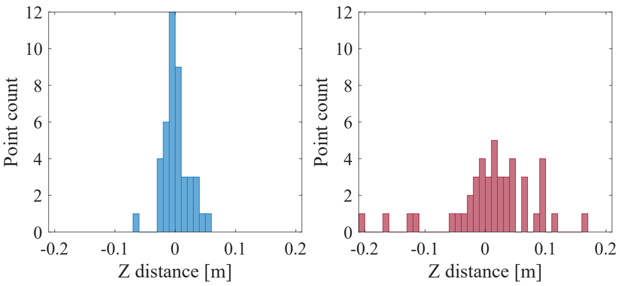

(a) Photogrammetry vs topography. (b) PLS vs topography.

Figure 8. Vertical error distributions obtained from point-to-point comparisons between the topographic control points and the site-scale photogrammetric dense cloud (a), and between the same topographic points and the SLAM-based PLS point cloud (b).

The comparison resulted in a mean vertical error of 0.002 m between the topographic survey and the photogrammetric point cloud, and 0.012 m between the topographic survey and the PLS dataset. The histograms highlight a near-zero mean error for both datasets. However, the PLS results exhibit a wider dispersion and a characteristic *doming effect*, with deviations increasing toward the extremities of the surveyed area and reaching values of up to approximately 0.20 m. This behavior is consistent with previously reported analyses obtained using the same SLAM-based PLS sensor under unconstrained conditions, as discussed in (Maset et al., 2021, Matellon et al., 2023). In contrast, the photogrammetric results confirm a higher level of vertical stability, with errors comparable to those observed in the CP-based accuracy assessment.

To further investigate precision and noise of the PLS point cloud, a local C2C analysis was performed at the scale of the individual temples. For the eastern temple, the C2C comparison yielded a mean distance of 0.040 m with a standard deviation of 0.036 m, while for the western temple the mean distance increased to 0.058 m with a standard deviation of 0.058 m. The higher values observed for the western temple are partly attributable to gaps in the photogrammetric reconstruction, particularly in the lower portions of stone blocks that were not fully captured by the UAV survey. Overall, the observed noise levels are in line with values reported in the literature for first-generation handheld SLAM systems, while more recent second-generation instruments demonstrate improved performance (Matellon et al., 2024, Teppati Losè et al., 2025).

4.3 Integrated Multi-Sensor Results

The final integrated point cloud highlights the complementary contribution of the two datasets at different spatial scales. As shown in Fig. 9, the overall site is represented by the continuous SLAM-based PLS dataset, while the areas corresponding to the two temples are characterized by a markedly higher level of geometric detail derived from the UAV photogrammetric reconstructions. The resulting model provides a spatially consistent representation of the archaeological area, combining full site coverage with detailed architectural information in correspondence with the preserved structures.

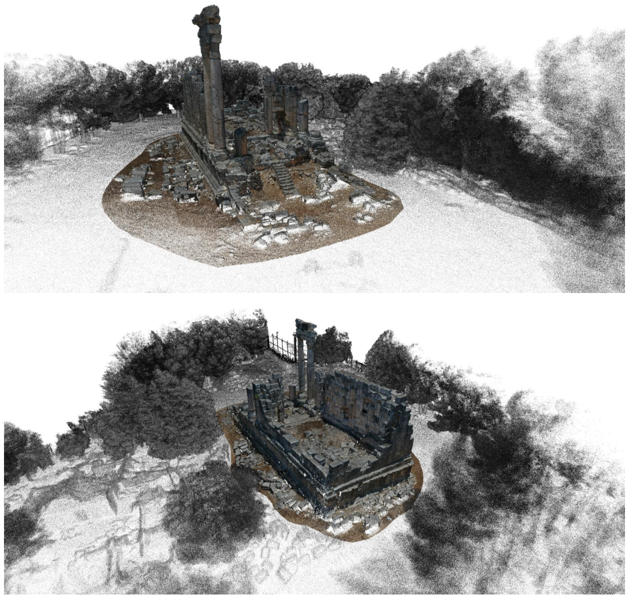

(a) Eastern temple and surroundings.

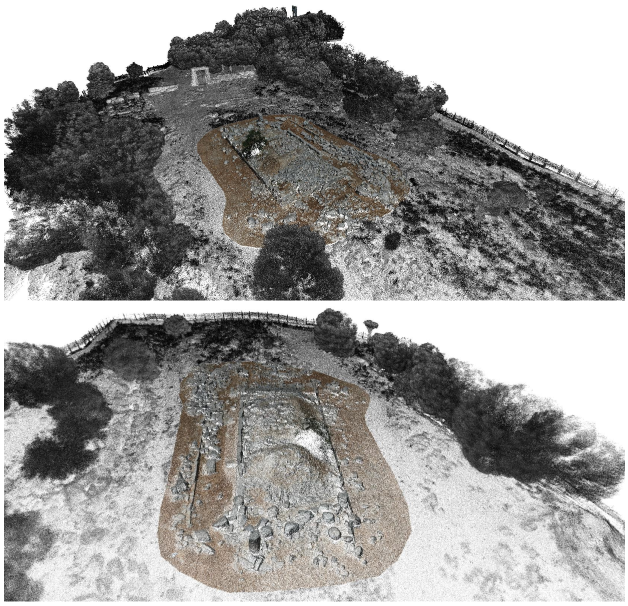

(b) Western temple and surroundings.

Figure 9. Integration of multi-sensor point clouds, combining close-range UAV photogrammetry for detailed temple reconstruction (shown in color) with the SLAM-based PLS dataset for full-site coverage (shown in grayscale according to intensity values).

5. Conclusion

This study demonstrated the effectiveness of integrating UAV photogrammetry and SLAM-based portable laser scanning for the comprehensive documentation of a large and morphologically complex archaeological site. The proposed multi-sensor workflow enabled the generation of a consistent, multi-scale 3D representation of the Qasr Naous area in the village of Ain Akrine (Lebanon), combining complete spatial coverage at the landscape scale with high-resolution architectural documentation of the Roman temples.

The results highlight the specific strengths and limitations of the adopted techniques. UAV photogrammetry provided high geometric accuracy and detailed surface modelling where visibility conditions were favorable, while the SLAM-based PLS survey proved particularly effective in densely vegetated and poorly accessible areas, allowing reliable ground modelling and the derivation of a site-wide DTM. The quantitative analyses confirmed that, despite the absence of external constraints, the SLAM-derived dataset achieved accuracy levels consistent with previously reported performance of the same sensor.

From a broader perspective, the proposed approach can be applied to a wide range of archaeological and cultural heritage contexts, provided that site-specific characteristics are appropriately taken into account. Dense vegetation strongly favors the adoption of LiDAR-based solutions, which remain essential for reliable ground modelling. Conversely, the availability of GNSS positioning would simplify topographic control and photogrammetric georeferencing, while only marginally affecting SLAM-based PLS surveys unless next-generation systems integrating GNSS measurements are employed. Overall, the presented results confirm that a carefully planned and integrated multi-sensor strategy can provide robust and versatile products supporting archaeological analysis, site management, and long-term conservation, even under challenging environmental and logistical conditions.

Acknowledgment

This research was financially supported by the Italian Ministry of Foreign Affairs and International Cooperation (MAECI 2025/3004 – Prot. n. 134854/109). The study was funded by the European Union – Next Generation EU (National Recovery and Resilience Plan, PNRR, Mission 4, Component 2, Investment 1.1, project code P2022LFYZJ). The authors gratefully acknowledge 3Dflow srl for providing the license of the 3DF Zephyr software. The authors also wish to thank Chiara Bozzi and Reem Nader for their valuable assistance during the field survey activities.

References

Aliquot, J., 2009. *La vie religieuse au Liban sous l'Empire Romain*. Presses de l'Ifpo, Beyrouth.

Chiabrando, F., Sammartano, G., Spanò, A., Spreafico, A., 2019. Hybrid 3D models: When geomatics innovations meet extensive built heritage complexes. *ISPRS International Journal of Geo-Information*, 8(3), 124.

Collart, P., Coupel, P., 1977. *Le petit autel de Baalbek*. P. Geuthner, Paris.

Conti, A., Pagliaricci, G., Bonora, V., Tucci, G., 2024. A comparison between terrestrial laser scanning and hand-held mobile mapping for the documentation of built heritage. *The International Archives of the Photogrammetry, Remote Sensing and Spatial Information Sciences*, 48, 141–147.

Di Stefano, F., Chiappini, S., Gorreja, A., Balestra, M., Pierdicca, R., 2021. Mobile 3D scan LiDAR: A literature review. *Geomatics, Natural Hazards and Risk*, 12(1), 2387–2429.

Donceel, R., 1966. Recherches et travaux archéologiques récents au Liban (1962-1965). *L'Antiquité classique*, 35, 238. https://www.persee.fr/doc/antiq_0770-2817_1967_num_36_1_2657.

Fassi, F., Dierna, M., Taffurelli, L., Helder, J. M., Fregonese, L., Vassena, G., 2025. Mobile mapping for architectural survey. The case of Doge's Palace in Venice: Challenges and lessons learn. *The International Archives of the Photogrammetry, Remote Sensing and Spatial Information Sciences*, 48, 457–464.

Hess, M., Ferreyra, C., 2021. Recording and comparing historic garden architecture. Value of SLAM-based recording for research on cultural landscapes in connection with heritage conservation. *The International Archives of the Photogrammetry, Remote Sensing and Spatial Information Sciences*, 46, 301–308.

Iamoni, M., Haider, M., Turri, L., Elias, A., Baldi, J. S., Vezzoli, V., in press. The 2018-2020 season report of the Northern Lebanon Project. The regional settlement of the inner plain of Koura. *BAAL*, 23, 307–331.

Iamoni, M., Haider, M., Turri, L., Simi, F., 2019. The Northern Lebanon project: Archaeological survey of the plain of Koura and the province of Tripoli. First season report. *BAAL*, 19, 147–172.

Krencker, D. M., Zschietzschmann, W., 1938. *Römische Tempel in Syrien, nach Aufnahmen und Untersuchungen von Mitgliedern der deutschen Baalbekexpedition 1901-1904*. De Gruyter, Berlin-Leipzig.

Masciotta, M. G., Sanchez-Aparicio, L. J., Oliveira, D. V., Gonzalez-Aguilera, D., 2023. Integration of laser scanning technologies and 360º photography for the digital documentation and management of cultural heritage buildings. *International Journal of Architectural Heritage*, 17(1), 56–75.

Maset, E., Cucchiaro, S., Cazorzi, F., Crosilla, F., Fusiello, A., Beinat, A., 2021. Investigating the performance of a handheld mobile mapping system in different outdoor scenarios. *The International Archives of the Photogrammetry, Remote Sensing and Spatial Information Sciences*, 43, 103–109.

Maset, E., Valente, R., Iamoni, M., Haider, M., Fusiello, A., 2022. Integration of photogrammetry and portable mobile mapping technology for 3D modeling of cultural heritage sites: The case study of the Bziza temple. *The International Archives of the Photogrammetry, Remote Sensing and Spatial Information Sciences*, 43(B2-2022), 831–837.

Maté-González, M. Á., Di Pietra, V., Piras, M., 2022. Evaluation of different LiDAR technologies for the documentation of forgotten cultural heritage under forest environments. *Sensors*, 22(16), 6314.

Matellon, A., Maset, E., Beinat, A., Visintini, D., 2024. Surface reconstruction from SLAM-based point clouds: Results from the datasets of the 2023 SIFET benchmark. *Remote Sensing*, 16(18), 3439.

Matellon, A., Maset, E., Visintini, D., Beinat, A., 2023. Feasibility and accuracy of as-built modelling from SLAM-based point clouds: Preliminary results. *The International Archives of the Photogrammetry, Remote Sensing and Spatial Information Sciences*, 48, 273–278.

Mendoza, M. A. D., De La Hoz Franco, E., Gómez, J. E. G., 2023. Technologies for the preservation of cultural heritage—a systematic review of the literature. *Sustainability*, 15(2), 1059.

Nordiguian, L., 2005. *Temples de l'époque romaine au Liban*. Presses de l'Université Saint-Joseph, Beyrouth.

Pepe, M., Alfio, V. S., Costantino, D., 2022. UAV platforms and the SfM-MVS approach in the 3D surveys and modelling: A review in the cultural heritage field. *Applied Sciences*, 12(24), 12886.

Perfetti, L., Vassena, G., Fassi, F., 2023. Preliminary survey of historic buildings with wearable mobile mapping systems and UAV photogrammetry. *The International Archives of the Photogrammetry, Remote Sensing and Spatial Information Sciences*, 48, 1217–1223.

Renan, E., 1864-1874. *Mission de Phénicie*. Imprimerie Imperiale, Paris.

Taylor, G., 1971. *The Roman temples of Lebanon/Les temples romains au Liban*. Dar el-Machreq, Beyrouth.

Teppati Losè, L., Rinaudo, F., Grasso, N., Bonfanti, C., Kappes, S., 2025. Moving toward the next generation of HMLS—Testing and validating the performances of second-generation SLAM systems compared to predecessors. *Sensors*, 25(8), 2488.

Zlot, R., Bosse, M., Greenop, K., Jarzab, Z., Juckes, E., Roberts, J., 2014. Efficiently capturing large, complex cultural heritage sites with a handheld mobile 3D laser mapping system. *Journal of Cultural Heritage*, 15(6), 670–678.